SEMARAK ILMU PUBLISHING

Journal of Advanced Research in Applied Mechanics

Journal homepage:
https://semarakilmu.com.my/journals/index.php/appl_mech/index
ISSN: 2289-7895

The Preheating Effect of Mild Steel Layers Deposited using SMAW at 100 A and 70 A

Ahmed Nazrin Md Idriss[1,*], Md Abdul Maleque[1], Zakiah Kamdi[2], Noorhafiza Muhammad[3], Azmir Azhari[4]

[1] Department of Manufacturing and Materials Engineering, Kulliyah of Engineering, International Islamic University of Malaysia, PO Box 10, 50728, Kuala Lumpur, Malaysia
[2] Department of Manufacturing Engineering, Faculty of Mechanical and Manufacturing Engineering, University Tun Hussein Onn Malaysia, 86400, Parit Raja, Batu Pahat, Johor, Malaysia
[3] Faculty of Mechanical Engineering Technology, University Malaysia Perlis, Kampus Tetap Pauh Putra, 26000, Arau, Perlis, Malaysia
[4] Faculty of Manufacturing and Mechatronic Engineering Technology, Universiti Malaysia Pahang Al-Sultan Abdullah, 26600 Pekan, Pahang, Malaysia

ARTICLE INFO

Article history:
Received 15 March 2024
Received in revised form 10 May 2024
Accepted 24 May 2024
Available online 30 June 2024

Keywords:
Mild steel; E6013; SMAW; preheat

ABSTRACT

In surface melting, preheating temperature is generally caused by the heat conduction through the substrate ahead of the molten pool and their presence help to increase the material dissolution. In this work comparative study was conducted to study the melt features of two samples produced at 100 A and 70 A using the shielded metal arc welding (SMAW) process. The effect of the preheating at 100 A and 70 A on the defects, melt dimensions, surface roughness, deposition rates and losses between samples were examined. It was found that all samples were free from crack, undercutting or lack of fusion suggesting selected processing conditions and material were successfully employed to hinder the problems. The clad at 100 A was associated with higher preheating temperatures and explained the reason to ease melt dissolution for finer rippling marks and surface roughness. The work demonstrated enormous spatter which was related to burning of the electrode coating and metal evaporation that had brought the deposition rate at 100 A similar at 0.15 g/sec to the low spatter 70 A track. Low heat input can be the foundation for building high clad thickness and more dilution through high energy input is preferable for joining.

1. Introduction

Over the years of developing surface melting using localized energy input processes [1], it came to realization that the preheating effect caused by dissipating heat from the thermal conduction played a crucial role to prolong melt solidification. To produce a crack free layer, preheating to the above critical temperature to render the residual stress is necessary for extending the cooling time [2]. The rise of preheating temperature ahead of the melt prow are responsible for the increase of melt geometry and dilution. The amount of porosity in the solidified melt pool was influenced by the

* *Corresponding author.*
E-mail address: ahmednazrin@gmail.com

https://doi.org/10.37934/aram.119.1.112120

preheating temperatures. Low strength was a result from high porosity content under tensile test [3]. The preheating effect from root track passes helped to increase the hardenability near the top layer using Ni- Mo electrode against HY80 high strength low alloy steel [4]. In a literature, the mechanical properties were influenced without and with 350^{o}C preheated temperature on cast ductile irons [5]. Welded samples that were not preheated or postheated showed better mechanical properties than those heat treated ones by shielded metal arc welding [6]. Rippling marks were formed by the vigorous solidifed melt waves and their sizes are influenced by heat inputs [7] Surface melting without preheating developed greater hardness than with preheatings [8]. The increased of welding current was found to increase the dilution percentages and hardness reduction of the alloyed steel [9]. Hardness developed at 20% more in the fusion zone than the mild steel substrate [10]. Multi-passes to develop a wall gave less dilution which was the reason for high hardness development [11]. Reinforced phases population, distribution and sizes were influenced by the preheating tempereatures [12-15].

Shielded metal arc welding (SMAW) is a high energy fusion process consisting deposited molten metal that is protected by the decomposed coating against oxidation. In terms of surface hardening or refurbishment, successful low wear and high hardness results were reported on excavator bucket teeth [16], continuos digest blade [17], tiller blade [18], valve seat [19] and mill roller [15]. Armor plates were joint using this method [20]. SMAW is used over than 50% in the welding industries [21]. In this work, the shielded metal arc was used to melt the E6013 electrode against the mild steel substrate at the 100 A and 70 A via oscillation or C-curve weaving technique. The reason to select this E6013 is because they do not differ that much in terms of chemical composition than those with the substrate. The possibility creating unprecedented defects can be hampered. The effect of preheating against defects, surface roughness, melt geometries, deposition rate and losses between the two tracks were compared and presented.

2. Experimental Work

The substrate used in the work was the mild steel cut to the dimension of 72 mm x 72 mm x 6 mm. This shielded metal arc process used the currents that was set at 100 A and 70 A to produce two single layer samples. The current used for melting the layers were from the recommendation of the supplier (Malaysian Oxygen; MOX). Miller Dialarc 250 AC/DC welding machine was used for the melting process. E6013 electrode with the diameter of 2.6 mm was used to weave on the separate substrate up to about 50 mm in length. Figure 1 shows the illustration of the curvy weaving pattern used to lay the molten metal as the electrode brought towards the end of the track. Before melting, a few strikes were employed on the surface of the mild steel to ensure a stable and continuous arc being generated. The chemical composition of the electrode and mild steel are shown in Table 1.

Table 1
Chemical composition of the E6013 electrode and the mild steel (wt %)

Material	C	Mn	Si	S	P	Cu	Fe
Electrode	0.07	0.45	0.35	0.010	0.010	Nil	Bal
Substrate	0.25 - 0.29	1.03	0.280	0.050	0.040	0.20	Bal

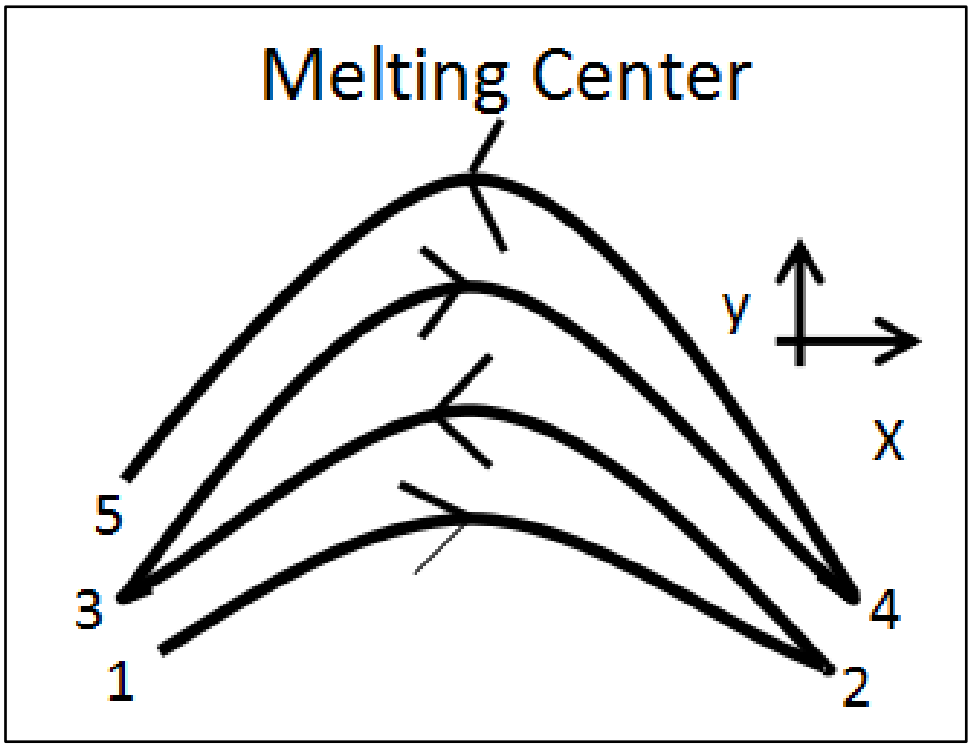

Fig. 1. Illustration describing the art of manipulating the curvy weaving technique. 1 to 5 are the transition points before weaving move to the opposing direction. Overlapping from point 2 to 3 partially remelts the previous layer associated with more of deposition along 1 to 2 while the other coincided to deposit only on the fresh substrate

Since this process was manually maneuvered, small variation electrode angle, speed or working distance inconsistencies forming the pattern may take place and so they were presumed negligible. Immediately after melting the slag was removed using chipping hammer. Both tracks topographies were observed at two different locations using DINO handheld microscope which was at the early and the later areas just before the deposition stops. The same microscope was used to measure the melt widths and heights where the technique for conducting this work is described in Figure 2. The melt widths were the distance between two metal edges from the top view. To measure the melt heights hot glue replication method was used to fabricate the contour of the substrate surface alongside the track as shown in Figure 2a. After the glue solidified, they were released from the sample and the melt height were taken from point (i) to (ii) as in Figure 2b. The surface roughness (Ra) was measured using Mitutoyo CS-3100 with the stylus dragged for 2 mm along the traverse direction of the melted layers. The deposition rate in Eq. (1) was calculated by dividing the substrate weight gained (SG_{wt}) over the recorded time (t) during melting. The substrate weight gained (SG_{wt}) was the value of substrate weight differences before and after the melting process. The deposition loss % was calculated using Eq. (2) Electrode loss denoted as EL_{wt} was calculated by substracting the weight of the electrode before than after the melting process. E_{wt} was the weight of the electrode. The process flow of this experimental work is described in Figure 3.

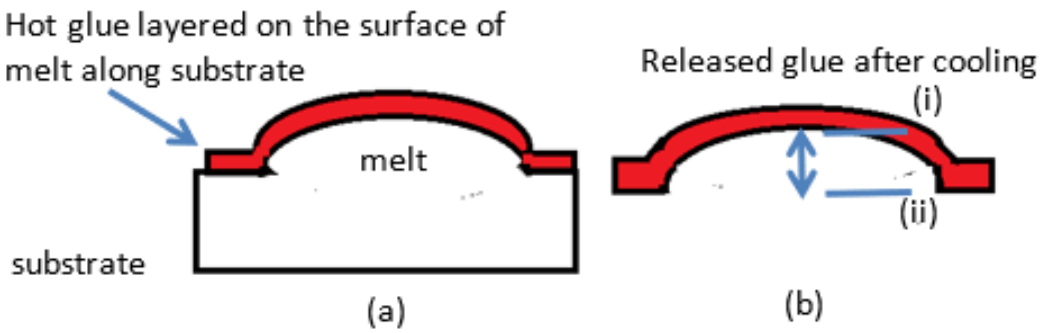

Fig. 2. Illustration describing the melt height measuring technique with (a) hot glue layered on the sample surface followed by (b) the distance of melt height from (i) to (ii)

$$Deposition\ rate = \frac{SG_{wt}}{t} \quad (1)$$

$$Deposition\ loss\ \% = \frac{EL_{wt} - SG_{wt}}{E_{wt}} \quad (2)$$

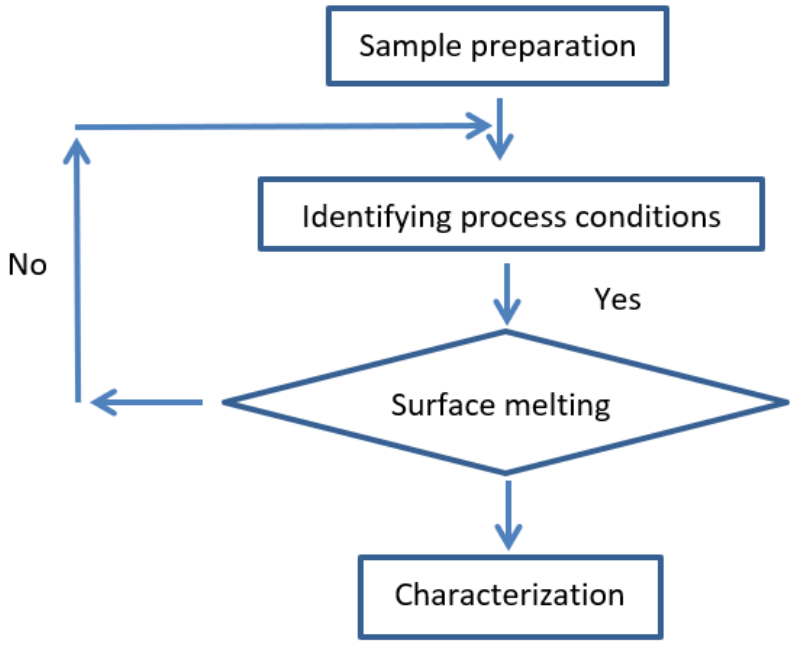

Fig. 3. The flow chart describing the experimental work

3. Results

The illustration describing the trajectory of the moving electrode resembling the curvy shape is shown in Figure 1. Number 1 to 5 depicts the transition point before the electrode moves to the next opposite direction. In the experimental work, partial remelting and reheating simultaneously took place along 2 to 1 when melting from point 2 to point 3. Partial remelting is deposited with metal from the electrode which happens at the overlapping layers. The other section of the molten pool which does not involve for overlappings, mix the liquid vigorously into the melt pool. As the melting electrode moves to the next numbers which are from point 3 to 4 followed by point 4 to 5, the substrate temperature gradually rises with the increased of metal deposition. This reciprocating

action lessens the melt front from confronting more of the cooler substrate and spreads the high temperature away from the electrode. It was reported that the mechanical properties were influenced by the difference of weaving pattern such as circular, triangular or sinusoidal under the gas metal arc welding (GMAW) [22]. In another work, Kumar and co-authors showed the dilution percentage was at 25.51% with a track produced by sinewave deposition technique while 27.07% and 30.05% were with linear and circular ones respectively [23]. These are the ways that generates the tempering effect and reduces the cooling rate while solidification. Tempering effect in welding is beneficial for the reduction of thermal generated stresses, improvising ductility or toughness. Preheating temperature near the end of the melted track of a single layer (without weaving) by TIG process recorded about 50^{o}C higher compared the early stage [24]. Under identical processing condition, the rise of the recorded steel substrate temperature was from 545^{o}C to 590^{o}C shielded with argon gas than between 970^{o}C to 1120^{o}C of helium [25].

The surface topography of the track layers at 100 A and 70 A with insets magnified at the early and later melting stages are shown in Figure 4. All tracks showed rippling marks indicating solidified melt waves upon metal deposition. The ripples produced at 100 A (Figure 4a i-iii) was rather smoother than at 70 A (Figure 4b iv-vi). It can also be seen that each track possessed rougher ripples during the early melting stage as shown in Figure 4ii, v than those before the melting stops in 4iii, vi. The Ra values were at 8.8 µm and 10.7 µm during the early melting stage for the 100 A and 70 A respectively. They were lower for both 100 A and 70 A at 5.5 µm and 6.4 µm respectively before melting stops. Visible and optical examination showed that no crack, under cutting or lack of fusion on any area in Figure 4. The contact angle was lesser than 90^{o} for both tracks which explained good bonding between the melt and the substrate took place during fusion. In the work, attempt at 60 A prevailed poor fusion and fabrication was not continued. Similarly, as TIG or laser processing that utilized shielding gasses such as argon or helium to protect against melt pool oxidation, SMAW depends on the electrode coating forming slag and gasses upon melting for similar oxidation protection on solidifying metal [12]. The tracks defect free are clear indication that wide range of processing energies can be used between recommended 100 A to 70 A to melt the E6013 electrode against steel surfaces.

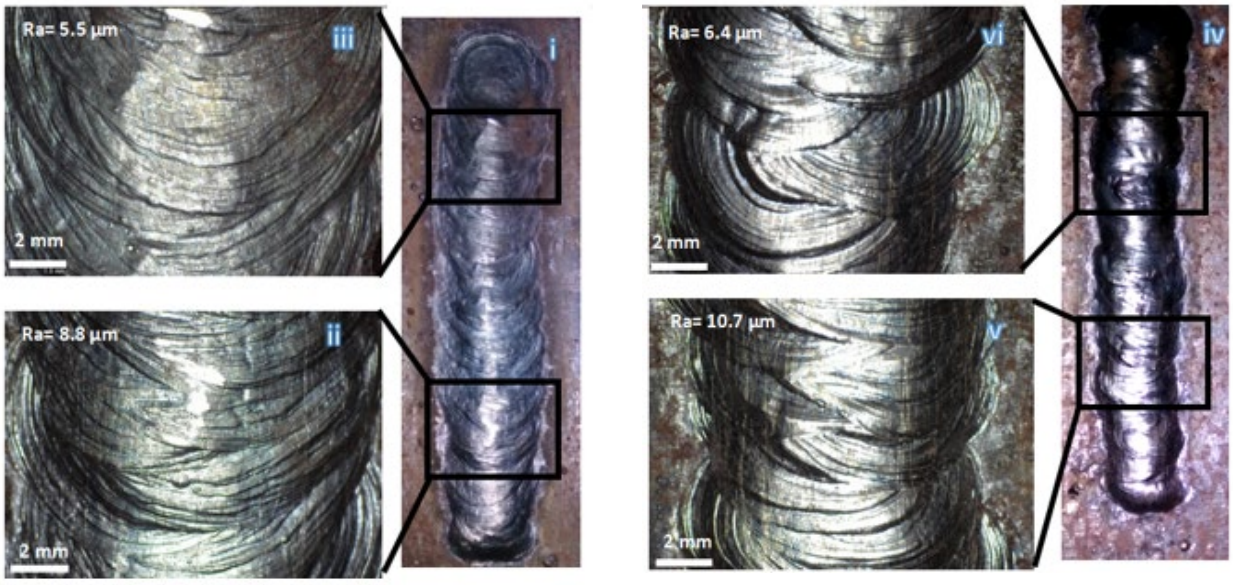

(a) (b)

Fig. 4. The surface topography of the produced tracks at using (a) 100 amp and (b) 70 amp withminsets locating the morphology of the rippling marks and roughness values

Rippling marks on the melt surface were not interfered by the floating slag during solidification which suggest that this low density and porous protective layer was apart from the metal. They were easily removed by chipping. Adding activated flux such as silicon oxide or chromium oxide produced slag than melting without flux and so with the electrode coating in this work [26] The rippling pattern follows the trajectory direction of the travelling electrode and their continuity is an evident that overlapping happened while weaving. The continuity of the melt track was also observed using sinewave technique under GMAW [23]. Because this work manipulated the curvy pattern, the overlapping distances vary from 2 to 1 as the electrode moved to the opposing point 2 to 3 and so with others (Figure 4). The melt temperature and turbulence were high and vigorous with 100 A leading for the surface to consist smooth ripples in Figure 4 (ii,iii). Fast solidification at the low melting temperature of 70 A gave higher viscosity of the molten metal which suddenly freezes for the rough and inconsistent rippling pattern in Figure 4v, vi. Research showed that the formation of rippling marks were associated from the stirring action of the melt that rapidly solidified as the heat source moved away from the molten pool. Rippling was observed on mild steel and stainless steel joint melted with and without activated flux under the TIG process [26] and others [27,28]. The low heat input representing fast solidification by TIG gave dull surface compared to heating at higher heat input that underwent more time to cool, revealing bright and shiny ripples [7].

This work also showed that the smoothest ripples were observed near the end of the melt track (Figure 4iii) than the early stage of melting at 100 A (Figure 4ii). They were also smoother at both corresponding locations compared to the 70 A (Figure 4v, vi). Region (Figure 4iii) may had acquired the highest preheating temperature which assist the melt to retain the lowest melt viscosity. Owing to this, the stirring action is presumed to be the most vigorous associated with more time needed to realize solidification. This resulted for the smoothest ripple with the Ra value of 5.5 µm (Figure 4iii) compared to the earlier one of 100 A with 8.8 µm (Figure 4ii). At 70 A, the later melting stage gave of 6.4 µm (Figure 4vi) while it was slightly higher at 10.7 µm (Figure 4v) just after the melting started proving rougher surface integrity than at 100 A. The reheating of the previous layers and the generation of the ahead preheating temperatures deposited using the curvy pattern were profound to create melt waves resulting finer ripples associated with lower roughness values. Not only that, the technique owns a credit to immune the melted track against the defect such as lack of fusion, undercutting or cracking.

The measured melt width and melt height results across the track both produced at 100 A and 70 A are shown in Figure 5 and Figure 6 respectively. The size of the melt geometry changes as melting progresses toward the end of the track. The graph shows that the width of the track produced at 100 A was greater at all track length between 9 mm to 12.2 mm than 7.5 mm to 9 mm of 70 A. This gave the width 100 A 1.3 times higher than at 70 A. The melt height was between 1.7 mm to 2.0 mm with the 70 A resulting 1.3 times higher than 100 A which was also observed by others [29]. Melting and preheating temperatures were higher at 100 A which had acquired greater melt width to accommodate the melt fluidity from the electrode at the expense of melt height than at 70 A. The fast solidification when 70 A was used gave greater melt height rather than facilitating the broadening of melt width. Nevertheless, the preheating effect showed its significance that gave higher dilution near the end from increased of melt width and reduced of melt height for both currents.

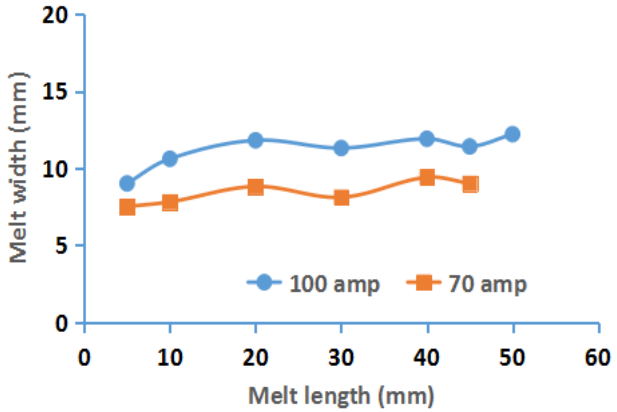

Fig. 5. The distances of the clad width against clad length with the 100 A and 70 A depositions

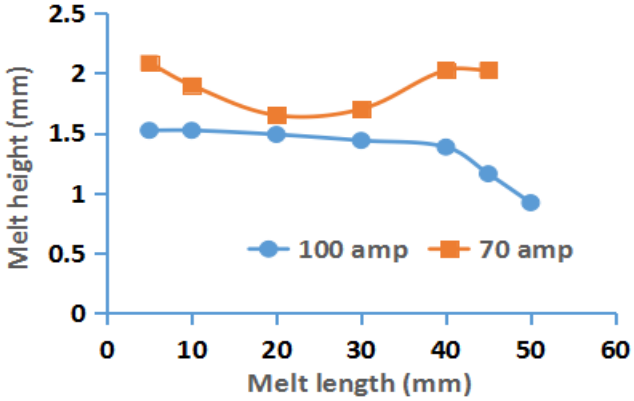

Fig. 6. The distances of the clad height against clad length with the 100 A and 70 A

During the experimental work, the observed spatter and plume were higher with the 100 A than at 70 A which one would think for greater deposition introduced into the molten pool when massive energy was utilized. However, after calculation using Eq. (1), the deposition rate was similar for both tracks at 0.15 g/sec showing no increased of higher amount of metal deployed into this single track at 100 A than at 70 A. This exemplified an overwhelming reduction of deposited material which had them lost in the form of spatter, burnt electrode coating and metal evaporation thus affecting the deposition rate. This is why the 100 A brought the deposited metal coincided to the value similar to the 70 A for both being at 0.15 g/sec. Higher current showed poor deposition rate than at the lower ones [30].

It has been reported that the generation of spatter increases with increased of heat input. Spatters up to the size of 2 mm was seen by the side of each track and their formation was explained for the reduction of deposited material into the track [31,32]. The similarity of the deposition rates at two current inputs giving 0.15 g/sec can be confirmed by the inverse proportion of the melt pool height and width as shown in Figure 5 and Figure 6. At 100 A, diluted metal spread to an average of 11 mm of width and 1.3 mm height. In contrast sudden solidification yield shorter width distance of 8.4mm at 70 A and mount the greater height at an average of 1.9 mm. Even so massive spatter generation was associated with high deposition losses during melting and additional work for their removal, processing at 100 A inherit high substrate dilution to join metal. Dissimilarly, the higher melt height fabricated at 70 A may suit to build melt thickness through overlappings [33,34].

4. Conclusions

Melted surfaces through the deposition of E6013 electrode on the surface of the mild steel substrate were successfully produced at 100 A and 70 A using shielded metal arc welding. Weaving the tracks using the C curve pattern consumed deposited metal that melts the substrate and partially remelts the previous layer that generates the tempering effect to slow the cooling time. The tracks consisted sizes of rippling marks and they were free from the crack, lack of fusion or undercutting defects. Massive spatter associated with burnt electrode covering and metal evaporation with the 100 A was concluded for the reduction of deposition rate to 0.15 g/sec similar to that the lower 70 A. The equal deposition rate is demonstrated via arbitrary melt pool geometric sizes by the wider spread of fused metal to an average of 11 mm of width and 1.3 mm of height for the 100 A and with the presence of fast solidification, the deposition laid 8.4 mm width with 1.9 mm built height at 70 A. In this work the low energy secures more of melt development at low dilution and imposing higher energy dilution is inevitable whilst favour to join metal.

Acknowledgement

The authors would like to thank Vocational College of Batu Lanchang, Penang, Malaysia for the technical assistance and providing the samples used in this work. The authors greatly acknowledge Department of Manufacturing & Materials Engineering of IIUM, Department of Manufacturing Engineering of UTHM and Faculty of Mechanical Engineering Technology, UniMaP for the technical supports and financial support from the Ministry of Higher Education Malaysia through FRGS/1/2019/TK03/UMP/02/25 (RDU1901161)

References

[1] Shibe, Vineet, and Vikas Chawla. "Combating Wear by Surface Modification Techniques." In *Proceedings of the International Conference on Research and Innovations in Mechanical Engineering: ICRIME-2013*, pp. 475-485. Springer India, 2014. https://doi.org/10.1007/978-81-322-1859-3_44

[2] Hu, C., and T. N. Baker. "Overlapping laser tracks to produce a continuous nitrided layer in Ti–6Al–4V alloy." *Journal of materials science* 32 (1997): 2821-2826.

[3] Zhu, Chenxiao, Xinhua Tang, Yuan He, Fenggui Lu, and Haichao Cui. "Effect of preheating on the defects and microstructure in NG-GMA welding of 5083 Al-alloy." *Journal of Materials Processing Technology* 251 (2018): 214-224. https://doi.org/10.1016/j.jmatprotec.2017.08.037

[4] Yayla, P. A. Ş. A., E. Kaluc, and K. Ural. "Effects of welding processes on the mechanical properties of HY 80 steel weldments." *Materials & design* 28, no. 6 (2007): 1898-1906. https://doi.org/10.1016/j.matdes.2006.03.028

[5] Pascual, M., J. Cembrero, F. Salas, and M. Pascual Martínez. "Analysis of the weldability of ductile iron." *Materials Letters* 62, no. 8-9 (2008): 1359-1362. https://doi.org/10.1016/j.matlet.2007.08.070

[6] de Jesus Jorge, Leandro, Verônica Scarpini Cândido, Alisson Clay Rios da Silva, Fabio da Costa Garcia Filho, Artur Camposo Pereira, Fernanda Santos da Luz, and Sergio Neves Monteiro. "Mechanical properties and microstructure of SMAW welded and thermically treated HSLA-80 steel." *Journal of materials research and technology* 7, no. 4 (2018): 598-605. https://doi.org/10.1016/j.jmrt.2018.08.007

[7] Mridha, Shahjahan, AN Md Idriss, and T. N. Baker. "Incorporation of TiC particulates on AISI 4340 low alloy steel surfaces via tungsten inert gas arc melting." *Advanced Materials Research* 445 (2012): 655-660. https://doi.org/10.4028/www.scientific.net/AMR.445.655

[8] Srikarun, Buntoeng, and Prapas Muangjunburee. "Wear Behavior of Hardfacing Deposits on 3.5% Chromium Cast Steel." *Key Engineering Materials* 658 (2015): 167-171. https://doi.org/10.4028/www.scientific.net/KEM.658.167

[9] Singh, Mandeep, Mohd Majid, M. A. Akhtar, Hitesh Arora, and Kapil Chawla. "Wear behaviour of SMAW hardfaced mild steel and influence of dilution upon hardfacing properties." *International Journal of Mechanical Engineering and Technology* 8, no. 7 (2017): 1652-1661.

[10] Pagare, Rohit, Dhanesh Awati, Shrinath Mane, Vijay Teli, and Amar Bhandare. "Investigating the Effects of Welding Parameters on Mild Steel by SMAW Technique." In *IOP Conference Series: Materials Science and Engineering*, vol. 998, no. 1, p. 012052. IOP Publishing, 2020. https://doi.org/10.1088/1757-899X/998/1/012052

[11] Sar, Mohammed Helan, Osamah Sabah Barrak, and Sabah Khammass Hussain. "Effect of multi-pass SMAW welding on the surface hardness and microstructure of carbon steel AISI 1050." In *IOP Conference Series: Materials Science and Engineering*, vol. 1105, no. 1, p. 012058. IOP Publishing, 2021. https://doi.org/10.1088/1757-899X/1105/1/012058

[12] Mridha, Shahjahan, A. N. Md Idriss, M. A. Maleque, I. I. Yaacob, and T. N. Baker. "Melting of multipass surface tracks in steel incorporating titanium carbide powders." *Materials Science and Technology* 31, no. 11 (2015): 1362-1369. https://doi.org/10.1179/1743284714Y.0000000712

[13] Choi, J., S. K. Choudhuri, and J. Mazumder. "Role of preheating and specific energy input on the evolution of microstructure and wear properties of laser clad Fe-Cr-CW alloys." *Journal of materials science* 35 (2000): 3213-3219. https://doi.org/10.1023/A:1004854801553

[14] Amuda, M. O. H., T. F. Lawal, K. S. Enumah, and Onitiri LL. "Influence of thermal treatments on sensitization in Cr-Mn-Cu austenitic stainless steel welds." *UNILAG Journal of Medicine, Science and Technology* 6, no. 2 (2018): 91-106.

[15] Buchanan, V. E., D. G. McCartney, and P. H. Shipway. "A comparison of the abrasive wear behaviour of iron-chromium based hardfaced coatings deposited by SMAW and electric arc spraying." *Wear* 264, no. 7-8 (2008): 542-549. https://doi.org/10.1016/j.wear.2007.04.008

[16] Singla, Shivali, Vineet Shibe, and J. S. Grewal. "Performance evaluation of hard faced excavator bucket teeth against abrasive wear using MMAW process." *International Journal of Mechanical Engineering Applications Research* 2, no. 02 (2011): 73-77.
[17] Tobi, AL Mohd, Z. Kamdi, M. I. Ismail, M. Nagentrau, L. N. H. Roslan, Z. Mohamad, A. S. Omar, and N. Abdul Latif. "Abrasive wear failure analysis of tungsten carbide hard facing on carbon steel blade." In *IOP Conference Series: Materials Science and Engineering*, vol. 165, no. 1, p. 012020. IOP Publishing, 2017. https://doi.org/10.1088/1757-899X/165/1/012020
[18] Kang, Amardeep Singh, Gurmeet Singh Cheema, and Shivali Singla. "Wear behavior of hardfacings on rotary tiller blades." *Procedia Engineering* 97 (2014): 1442-1451. https://doi.org/10.1016/j.proeng.2014.12.426
[19] Selvi, S., S. P. Sankaran, and R. Srivatsavan. "Comparative study of hardfacing of valve seat ring using MMAW process." *Journal of materials Processing technology* 207, no. 1-3 (2008): 356-362. https://doi.org/10.1016/j.jmatprotec.2008.06.053
[20] Balakrishnan, M., V. Balasubramanian, G. Madhusuhan Reddy, and K. Sivakumar. "Effect of buttering and hardfacing on ballistic performance of shielded metal arc welded armour steel joints." *Materials & Design* 32, no. 2 (2011): 469-479. https://doi.org/10.1016/j.matdes.2010.08.037
[21] Kalpakjian, Serope, and Steven R. Schmid. "Manufacturing engineering." *Technology; Prentice Hall: London, UK* (2009): 568-571.
[22] Guzman-Flores, Isidro, Benjamin Vargas-Arista, Juan Jose Gasca-Dominguez, Celso Eduardo Cruz-Gonzalez, Marco Antonio González-Albarrán, and Joaquin del Prado-Villasana. "Effect of torch weaving on the microstructure, tensile and impact resistances, and fracture of the HAZ and weld bead by robotic GMAW process on ASTM A36 steel." *Soldagem & Inspeção* 22, no. 1 (2017): 72-86. https://doi.org/10.1590/0104-9224/si2201.08
[23] Kumar, N. Pravin, and N. Siva Shanmugam. "Some studies on nickel based Inconel 625 hard overlays on AISI 316L plate by gas metal arc welding based hardfacing process." *Wear* 456 (2020): 203394. https://doi.org/10.1016/j.wear.2020.203394
[24] Muñoz-Escalona, P., S. Mridha, and T. N. Baker. "Effect of silicon carbide particle size on microstructure and properties of a coating layer on steel produced by TIG technique." *Advances in Materials and Processing Technologies* 2, no. 4 (2016): 451-460. https://doi.org/10.1080/2374068X.2016.1246217
[25] Muñoz-Escalona, P., Shahjahan Mridha, and T. N. Baker. "Effect of shielding gas on the properties and microstructure of melted steel surface using a TIG torch." *Advances in Materials and Processing Technologies* 1, no. 3-4 (2015): 435-443. https://doi.org/10.1080/2374068X.2015.1133789
[26] Kuo, Cheng Hsien, Kuang Hung Tseng, and Chang Pin Chou. "Effect of activated TIG flux on performance of dissimilar welds between mild steel and stainless steel." *Key Engineering Materials* 479 (2011): 74-80. https://doi.org/10.4028/www.scientific.net/KEM.479.74
[27] Wang, X. H., S. L. Song, Z. D. Zou, and S. Y. Qu. "Fabricating TiC particles reinforced Fe-based composite coatings produced by GTAW multi-layers melting process." *Materials Science and Engineering: A* 441, no. 1-2 (2006): 60-67. https://doi.org/10.1016/j.msea.2006.06.015
[28] Bandhu, Din, Faramarz Djavanroodi, G. Shaikshavali, Jay J. Vora, Kumar Abhishek, Ashish Thakur, Soni Kumari, Kuldeep K. Saxena, Mahmoud Ebrahimi, and Shokouh Attarilar. "Effect of metal-cored filler wire on surface morphology and micro-hardness of regulated metal deposition welded ASTM A387-Gr. 11-Cl. 2 steel plates." *Materials* 15, no. 19 (2022): 6661. https://doi.org/10.3390/ma15196661
[29] Sandhu, Sandeep Singh, and A. S. Shahi. "Metallurgical, wear and fatigue performance of Inconel 625 weld claddings." *Journal of Materials Processing Technology* 233 (2016): 1-8. https://doi.org/10.1016/j.jmatprotec.2016.02.010
[30] Crespo, Amado Cruz, Americo Scotti, and Manuel Rodriguez Perez. "Operational behavior assesment of coated tubular electrodes for SMAW hardfacing." *Journal of materials processing technology* 199, no. 1-3 (2008): 265-273. https://doi.org/10.1016/j.jmatprotec.2007.07.048
[31] Kataoka, Tokihiko, Rinsei Ikeda, and Koichi Yasuda. "Development of ultra-low spatter CO2 gas-shielded arc welding process "J-STAR® Welding"." *JFE Tech Rep* 10 (2007): 31-34.
[32] Murayama, Masatoshi, Daisuke Oazamoto, and K. Ooe. "Narrow gap gas metal arc (GMA) welding technologies." *JFE Technol. Rep* 20 (2015): 147-153.
[33] Sexton, L., S. Lavin, G. Byrne, and A. Kennedy. "Laser cladding of aerospace materials." *Journal of Materials Processing Technology* 122, no. 1 (2002): 63-68. https://doi.org/10.1016/S0924-0136(01)01121-9
[34] Kaierle, Stefan, Ludger Overmeyer, Irene Alfred, Boris Rottwinkel, Jörg Hermsdorf, Volker Wesling, and Nils Weidlich. "Single-crystal turbine blade tip repair by laser cladding and remelting." *CIRP Journal of Manufacturing Science and Technology* 19 (2017): 196-199. https://doi.org/10.1016/j.cirpj.2017.04.001